

# Heating Events in the Quiet Solar Corona

Säm KRUCKER<sup>1</sup> and Arnold O. BENZ<sup>2</sup>

<sup>1</sup>*Space Sciences Laboratory, University of California, Berkeley CA 94720, USA*

<sup>2</sup>*Institute of Astronomy, ETH-Zentrum, CH-8092 Zürich, Switzerland*

*E-mail(SK): krucker@ssl.berkeley.edu*

## Abstract

Sensitive observations of the quiet Sun provided by (1) the SXT on board the Yohkoh satellite, (2) the EIT on board the SoHO spacecraft in high-temperature iron line emission, and (3) the Very Large Array (VLA) in the centimeter radio range are investigated in view of the coronal heating problem. The observed enhancements in coronal emission measure are interpreted as heating events (microflares) bringing chromospheric material to coronal temperatures, whereas the radio observations show the existence of non-thermal emission related to some of these heating events. Assuming an effective height of 5000 km, the thermal energy inputs by such microflares have been found in the range from  $8 \times 10^{24}$  erg to  $1.6 \times 10^{26}$  erg, and the total energy input amounts to about 16% of the average radiated power of the coronal plasma in the quiet corona. The frequency distribution of microflares is an approximate power-law of the form  $f(E) = f_0 E^{-\delta}$  with a power-law index  $\delta$  between 2.3 and 2.6. As the low-energy cutoff is due to sensitivity limitations and the power-law index is steeper than 2, these observations demonstrate the possibility that microflares dominate the energy input into the quiet corona.

**Key words:** Sun: activity — Sun: corona — Sun: flare — Sun: X-rays — Sun: radio

## 1. Introduction

The heating of the corona is one of the persisting enigmas of the Sun. Although several explanations for the million degree outer atmosphere have been proposed, none has been confirmed (e.g. reviews in Ulmschneider et al. 1991). The high temperature of the solar corona was originally interpreted by the dissipation of various kinds of waves originating at lower layers. More than a decade ago heating by a myriad of small flares releasing magnetic energy by reconnection has been proposed (Levine 1974; Priest 1981; Parker 1983). However, the suggested microflares or nanoflares have not yet been identified.

An obvious requirement to explain coronal heating is that the energy input by microflares is sufficient to balance the radiation loss of the corona. The energy input has been evaluated by intergrating in energy the rate of flare energy release,  $f(E)$ , observed at the energy  $E$  per unit area. Thus the flare input power is

$$P = \int_{E_{\min}}^{E_{\max}} E f(E) dE \quad [\text{erg s}^{-1} \text{cm}^{-2}]. \quad (1)$$

The minimum energy  $E_{\min}$  is usually set by instrumental limits, and the maximum energy  $E_{\max}$  by some high-energy cutoff or the largest flare that occurred in the observing period. If the distribution of the thermal energy is a power law,  $f(E) = f_0 E^{-\delta}$ , the integral in Eq. (1) behaves differently depending on  $\delta$  being larger or smaller than 2: If  $\delta > 2$  and  $E_{\min} \ll E_{\max}$ , the result is

$$P \approx \frac{f_0}{\delta - 2} \frac{1}{E_{\min}^{\delta-2}}. \quad (2)$$

$P$  is dominated by the low-energy part of the energy range. The reverse holds if  $\delta < 2$ .

An additional requirement to explain coronal heating is that the heating must be stronger where the radiative losses are observed to be enhanced. This topic is not discussed in this paper. However, it is mentioned that Benz & Krucker (1998) indeed found a linear relation between the thermal energy input by microflares and the radiative

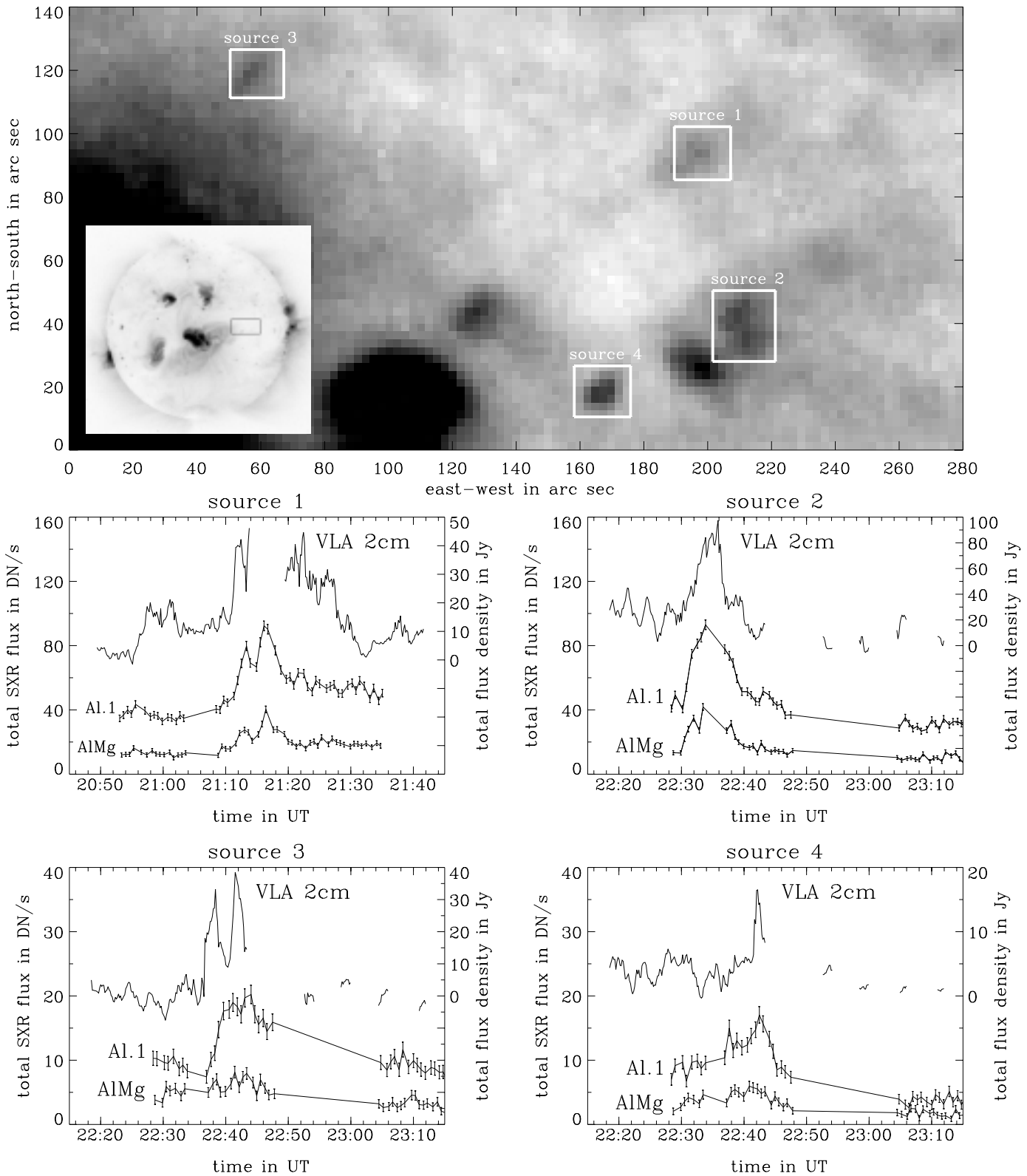


Fig. 1.. Temporal evolution of microflares observed in soft X-rays and radio waves. The image at the top shows the averaged SXR flux on February 20, 1995 in the quiet corona. The location of the field of view is indicated by a rectangular frame in the full disk image presented in the left corner. Enhanced flux is shown dark. The locations of the network flares are indicated by boxes. The plots below show the temporal variations of the SXR flux in the Al.1 filter and AlMg filter (the contribution of the scattered light has been subtracted) and the radio flux at 2.0 cm for the different network flares.

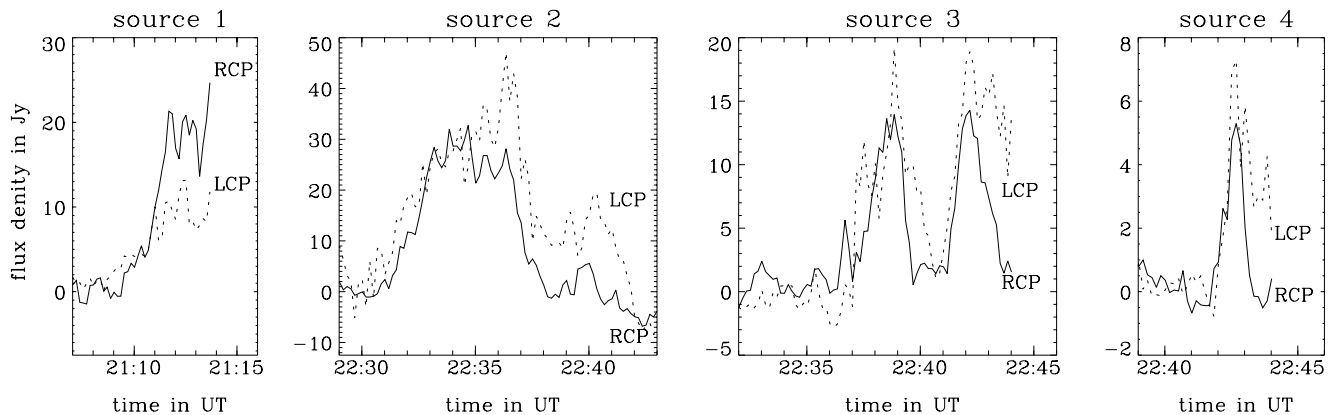


Fig. 2.. The right circularly polarized (RCP, solid curve) and the left circularly polarized (LCP, dotted curve) components of the flux density of the radio microflares presented in Figure 1.

losses of identical picture elements observed in the quiet corona.

For regular flares (generally located in *active regions*), the observations have mostly been analyzed by peak flux or peak count rate measurements. The results are power-law distributions with indices  $\delta$  around 1.8 (Datlowe et al. 1974; Lin et al. 1984; Dennis 1985; summarized by Crosby et al. 1993). The latter authors also present a substantial investigation on the total energy in flare electrons observed in hard X-ray bremsstrahlung, finding  $\delta = 1.53 \pm 0.02$ .

Soft X-ray peak fluxes of regular flares have a power-law index between 1.84 (Hudson et al. 1969) and 1.75 (Drake 1971). The latter author reports an exponent of the fluence (time-integrated flux, proportional to the total radiated flare energy) of 1.44. Shimizu (1995) finds a power-law index between 1.5 and 1.6 for flare thermal energy inputs larger than  $10^{27}$  erg as determined from soft X-ray brightenings in active regions. He estimates that the energy supplied by these small flares is at most 20% of the required amount to heat the corona in active regions. The flat distribution ( $\delta < 2$ ) suggests that the flares below the sensitivity limit cannot be responsible for the rest.

If flares heat the corona, they must be not only smaller (microflares), but more numerous. Thus, their power-law index must exceed 2. Vlahos et al. (1995) have simulated the coronal energy release by avalanche models. Their anisotropic version predicts small flares having a power-law index of 3.5.

The present paper is a summary of our work on microflare heating we have done so far. For more details the reader is referred to the already published papers. A general review of SXR transient activities is present by Shimizu (this proceeding). In this work, the question of coronal heating in *quiet regions* is investigated using soft X-ray (Yohkoh/SXT) and high-temperature iron lines in EUV (SoHO/EIT) that originate directly from the corona. Imaging radio observations (VLA) are additionally used to look for non-thermal emissions occurring simultaneously during the coronal SXR/EUV brightenings. First, the results obtained by analyzing single events are summarized followed by some comments about the observed microflare frequency distribution.

## 2. Single event analysis

Small soft X-ray (SXR) microflares above the network of the quiet Sun have been discovered by Krucker et al. (1997). Figure 1 shows the temporal evolution of the total SXR flux during four microflares. The brightenings are caused mostly by an increase of the coronal emission measure. The observed coronal temperature increases only slightly during these X-ray events. Thus the increase in coronal emission measure (square of density times volume) can be interpreted as evaporation events similar to regular flares in active regions. This was supported by the observation of associated radio emissions, some of which peaked before the soft X-rays (cf. Figure 1) and were polarized (cf. Figure 2), and thus were possibly of non-thermal origin. Except for the low temperature, these properties are typical for regular flares, supporting the interpretation of soft X-ray brightenings as microflares. The energy input can be readily estimated from the thermal energy of the newly heated material injected into the corona.

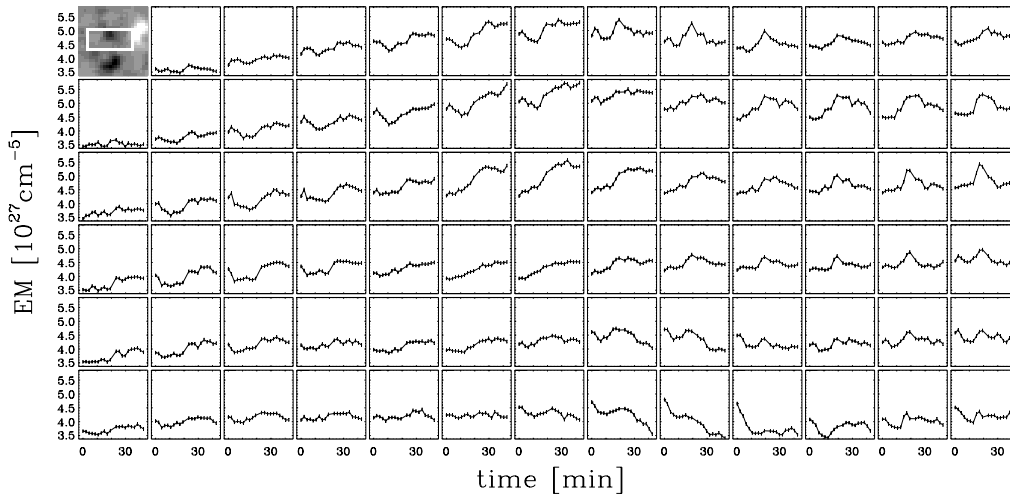


Fig. 3.. Coronal emission measure vs. time for single, adjacent pixels, each having a size of  $2.6'' \times 2.6''$ . A typical sample of only 77 out of the total number of 23800 pixels observed on July 12, 1996 are shown. The error bars are conservative upper limits. In the upper left corner the displayed area (quiet region) is marked on a magnetogram (SoHO/MDI data).

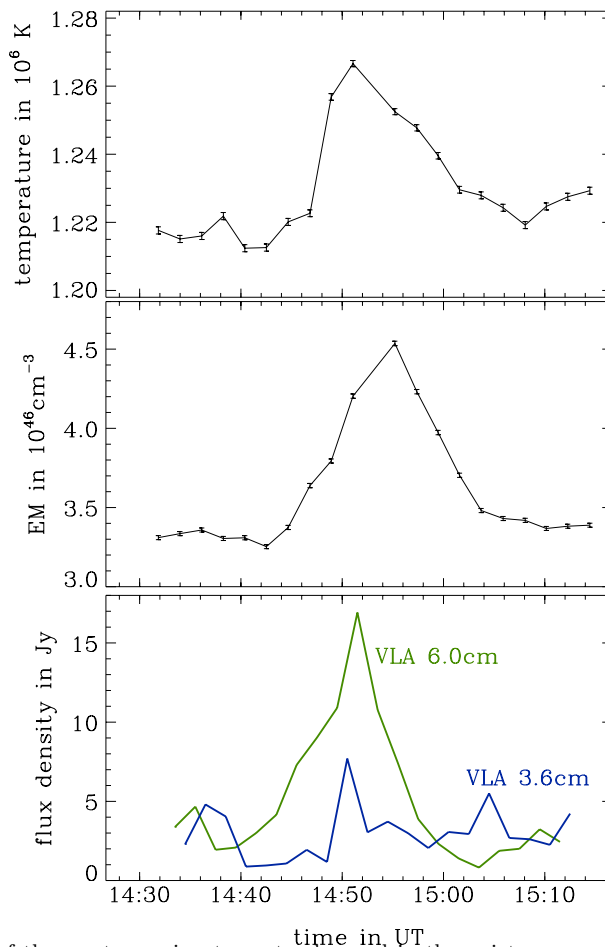


Fig. 4.. Time profile of one of the most prominent events observed in the quiet corona. Top: average temperature (formal value) over the area of enhanced intensity; no background was subtracted. Subtracting the pre-existing background emission of the plasma present before the enhancement, the peak temperature reaches a more realistic value of  $1.44(\pm 0.03) \cdot 10^6$  K (cf. Benz & Krucker 1998). Middle: total emission measure of the same area in the  $1 - 2 \cdot 10^6$  K temperature range. Bottom: radio flux density observed simultaneously by the VLA at 6 and 3.6 cm wavelength.

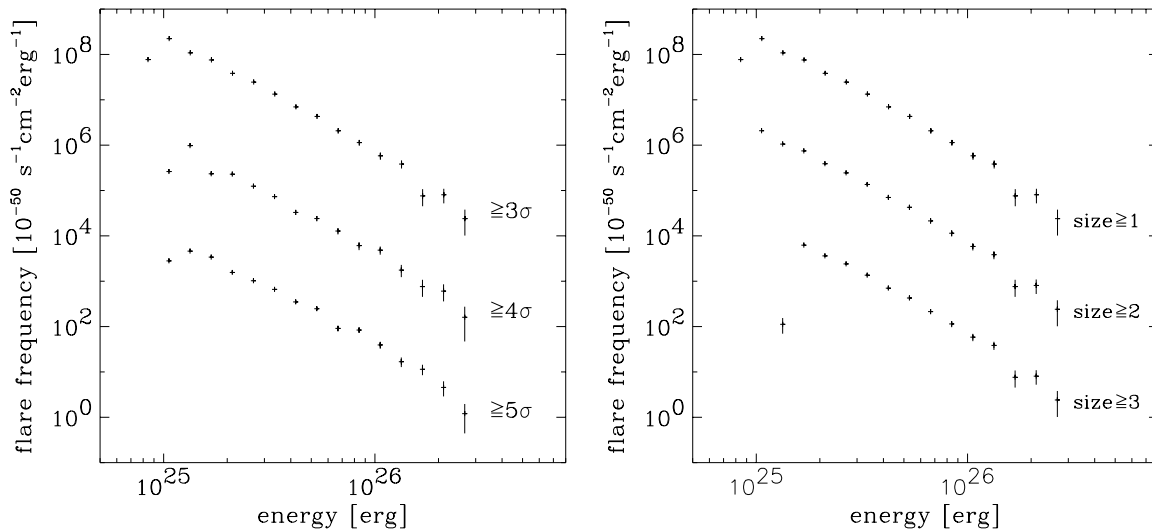


Fig. 5. The number of flares per unit time, area, and energy is shown vs. thermal flare energy. The error bars (vertical) indicate the statistical error due to the number counting. (*Left*): Three versions are displayed with minimum peak enhancement of the emission measure by 3, 4, and 5  $\sigma$ . They are offset subsequently by a factor 100. The power-law approximation to the flat part of the log-log-distribution of  $\geq 3\sigma$  events is  $f(E) = f_0 E^{-2.59}$ . — (*right*): Similar to the version on the left for  $\geq 3\sigma$  events. In addition, a requirement on minimum event area has been introduced. Three versions are displayed with minimum event area of one pixel (same as on the left), 2, and 3 pixels. They are offset subsequently by a factor 100.

They have a typical thermal energy content of  $10^{26}$  erg per event and occur at a rate of 1200 events per hour over the whole Sun. The energy was calculated from the thermal energy content assuming a filling factor of unity. For incomplete filling, the energy must be reduced by the square root of the filling factor.

More recently, the coronal emission measure in quiet regions has been observed in coronal EUV iron lines (SoHO/EIT) and was found to fluctuate locally at time scales of a few minutes in a large majority of pixels (Benz & Krucker 1998, 1999, cf. Figure 3). The analysis of the most prominent events confirms the results found earlier in Yohkoh SXR observations (Benz & Krucker 1998). The higher count rates at EUV wavelengths allow now to follow the temporal evolution of the derived temperature and emission measure (Figure 4). Often the maximum temperature precedes the emission measure peak suggesting impulsive and rapid heating early in the event. In regular flares several orders of magnitude more powerful, this is a well-known property. The spatially coincident radio emission shown in Figure 4 peaks simultaneously with the temperature time profile and has a decreasing spectrum in frequency. A decreasing spectrum is compatible with synchrotron emission as observed during regular flares. However, about half of the observed radio sources related to EUV brightenings show increasing spectra compatible with thermal emission.

### 3. Statistical analysis

Krucker & Benz 1998 determined several methods to approximate the flare frequency distribution of microflares observed in the quiet corona. They found that the energy distribution of the enhancements is an approximate power law with an index between 2.3 and 2.6 (cf. Figure 5). At low energies, about  $10^{25}$  erg, the distribution is cut by limited sensitivity. For such a power-law distribution with index above 2, the derived thermal energy input is limited by the low-energy cutoff and is a lower limit. The observed  $\geq 3\sigma$  events in coronal emission measure enhancements constitute about 16% of the required energy to create the quiet corona and radiate the observed emission. Since the distribution is cut by limited sensitivity, the value is a lower limit to the total energy input, but is also model dependent. However, the observation of a relatively steep power-law slope is more important than the derived fraction of the microflare energy input. Due to this steep index of more than 2, it cannot be excluded that enhancements smaller than the sensitivity limit of these observations constitute the major energy input. Assuming an effective height of 5000 km, the observed power law would have to continue to about  $3 \times 10^{23}$  erg, comprising about 28000 microflares per second on the whole Sun, to match the observed radiation loss.

A similar analysis of the flare frequency distribution of EUV microflares observed by EIT is presented by Berghmans et al. (1998). They found a power law index below 2. Instead of the thermal energy, as used in this work, the

total observed radiative losses are used as an approximation of the input provided by microflares. Radiative losses are proportional to the observed emission measure enhancements times duration, whereas thermal energies are proportional to the square root of the emission measure enhancements. Next to the much lower number of flares analysed by Berghmans et al., a further difference between these two works is the determined source sizes of the largest flares. In this work, the algorithm to determine flare sizes gives sizes up to  $50 \text{ Mm}^2$ , whereas the algorithm used by Berghmans et al. gives several microflares with size of  $250 \text{ Mm}^2$ . Single event analysis as presented in Section 2 show source sizes of the largest flares around  $50 \text{ Mm}^2$ .

#### 4. Conclusions

Enhancements in coronal emission measure have been observed and interpreted as heating events by microflares. The observed enhancements suggest that the corona is not only heated, but plasma is frequently and impulsively injected from the chromosphere. Thus coronal heating may actively involve the chromosphere as a supplier of material. The microflare frequency distribution is found to be a power law with a slope steeper than 2, thus emphasizing the importance of even smaller events below the present detection limits.

#### References

- Benz A.O., Krucker S. 1998, *Solar Phys.*, 182, 349  
Benz A.O., Krucker S. 1999, *A&A*, 341, 286  
Berghmans, D., Clette, F., Moses, D. 1998, *A&A*, 336, 1039  
Crosby N.B., Aschwanden M.J., Dennis B.R. 1993, *Solar Phys.* 143, 275  
Datlowe D.W., Elcan M.J., Hudson H.S. 1974, *Solar Phys.* 39, 155  
Dennis B.R. 1985, *Solar Phys.* 100, 489  
Drake J.F. 1971, *Solar Phys.* 16, 152  
Hudson H.S., Peterson L.E., Schwartz D.A. 1969, *ApJ* 157, 389  
Krucker S., Benz A.O., Acton L.W., Bastian T.S. 1997a, *ApJ* 488, 499  
Krucker S., Benz A.O. 1998, *ApJL* 501, L216  
Levine, R.H. 1974, *ApJ* 190, 447  
Lin R.P., Schwartz R.A., Kane S.R., Pelling R.M., Hurley K.C. 1984, *ApJ* 283, 421  
Parker, E.N. 1983, *ApJ* 264, 635  
Priest, E.R. 1981, *Solar Flare Magnetodynamics*, Gordon & Breach, London  
Shimizu T. 1995, *PASJ* 47, 251  
Ulmschneider P., Rosner R., Priest, E.R. (eds.) 1991, *Mechanisms of chromospheric and coronal heating*, Springer-Verlag, Berlin  
Vlahos L., Georgoulis M., Kluiving R., Paschos P. 1995, *A&A* 299, 897